



ACADEMIC
PRESS

Available online at www.sciencedirect.com

SCIENCE @ DIRECT®

Journal of Magnetic Resonance 159 (2002) 145–150

JMR

Journal of
Magnetic Resonance

www.academicpress.com

3D HSQC-HSQMBC—increasing the resolution of long-range proton–carbon correlation experiments[☆]

Dušan Uhrín^{*}

University of Edinburgh, Department of Chemistry, Joseph Black Chemistry Building, West Mains Road, Edinburgh EH9 3JJ, UK

Received 13 May 2002; revised 9 September 2002

Abstract

A 3D HSQC-HSQMBC experiment is proposed for increasing the separation of proton–carbon long-range correlation cross peaks, the lack of which is occasionally seen in corresponding 2D experiments. It is aimed at complex molecules with many protonated carbons exhibiting a narrow spread of ¹³C chemical shifts e.g., complex carbohydrates. It does not yield long-range correlation of quaternary carbons. An extra indirectly detected ¹H dimension of this experiment provides additional separation of long-range correlation cross peaks by utilising the chemical shifts of protons directly attached to ¹³C. Evolution of single-quantum coherences throughout the entire pulse sequence ensures that the cross peaks are inphase pure absorption singlets in both indirectly detected dimensions, thus maximising the resolution and sensitivity of the experiment. Partial signal cancellation can be expected due to the antiphase character of peaks in the directly detected dimension. The intensity of cross peaks depends on the length of a single long-range evolution interval and values of both active and passive long-range coupling constants of each carbon. The 3D HSQC-HSQMBC experiment provided high quality long-range correlation spectra of a 2 mg pentasaccharide sample in 27 h. The technique can also be used for measurement of long-range heteronuclear coupling constants from pure antiphase multiplets in the directly detected dimension.

© 2002 Elsevier Science (USA). All rights reserved.

Keywords: Proton–carbon long-range correlation; 3D; HSQMBC; Carbohydrates

1. Introduction

Proton–carbon chemical shift correlation via one-bond and long-range coupling constants is essential for structure determination of small and medium size molecules by NMR spectroscopy. Usually two separate 2D experiments, optimised for one-bond [1,2] and long-range [3] heteronuclear interactions, are acquired in order to establish unambiguously both types of interactions. In 2D ¹H-detected heterocorrelated correlated experiments the cross peaks may occasionally show lack of separation in the indirectly detected ¹³C dimension, which may cause ambiguities during the assignment of long-range correlated spectra. It has been recognised that additional signal dispersion can be achieved by

adding a third dimension to 2D long-range correlation experiments by utilising the one-bond heteronuclear correlation [4]. In their experiment, Hernández and LeMaster [4] used the proton–carbon long-range evolution interval to encode simultaneously the proton chemical shifts, transferred the magnetisation to ¹³C, refocused the long-range couplings, labelled the ¹³C chemical shift in a variable time manner and finally back-transferred the magnetisation to protons via one-bond coupling constants in a sensitivity-enhanced HSQC step. We present here a different implementation of the same principle and propose a new 3D experiment for increased separation of proton–carbon long-range correlation cross peaks of protonated carbons.

2. Results and discussion

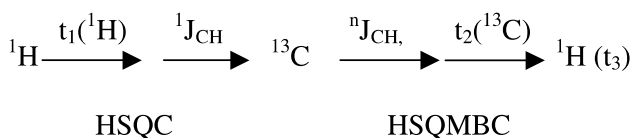
The proposed experiment starts with a variable time ¹H chemical shift-labelling period (*t*₁) followed by an

[☆]The pulse sequence presented in this article can be downloaded from <http://www.bionmr.chem.ed.ac.uk/~dusan/pulse.html>.

^{*}Fax: +44-131-650-7155.

E-mail address: dusan@chem.ed.ac.uk.

INEPT transfer optimised for $^1J_{\text{CH}}$ coupling constants. Once the magnetisation has been transferred to ^{13}C , the antiphase magnetisation with respect to $^nJ_{\text{CH}}$ is created, the $^1J_{\text{CH}}$ couplings are refocused and the ^{13}C chemical shifts are labelled (t_2). The magnetisation is then transferred to long-range coupled protons and detected during t_3 . Such magnetisation transfer pathway was previously utilised in several 2D [5,6] and 3D [7] long-range correlation experiments. The flow of magnetisation in the resulting 3D HSQC-HSQMBC experiment can be schematically depicted as



where HSQMBC stands for Heteronuclear Single-Quantum Multiple-Bond Correlation [8–11].

Both parts constituting this pulse sequence can be designed in several ways. Two implementations for each of the HSQC (Fig. 1a, b) and HSQMBC (Fig. 1c, d) parts are discussed here. The experiment starts with a variable time proton chemical-shift period, t_1 . In scheme A, the $\text{BIRD}^{\text{r,X}}$ pulse [12] is applied amid this interval.

This pulse inverts only protons attached to ^{12}C (r , remote protons) and ^{13}C nuclei (X) thus effectively eliminating the evolution of proton–proton coupling constants of ^1H – ^{13}C protons while allowing for their chemical shift labelling during t_1 [13]. In practice, such simplification of multiplets becomes significant only for t_1 acquisition times $>0.5/J_{\text{HH}}$. Nonetheless, when the $\text{BIRD}^{\text{r,X}}$ pulse is surrounded by pulsed-field gradients of opposite polarity [14] a substantial reduction of cancellation artefacts originating from remote protons is achieved [15] (compare Fig. 2a and b). The use of this G-BIRD block [14] is therefore recommended regardless of the length of the t_1 acquisition time. Together with additional purging pulsed-field gradients [16] and a basic 2-scan phase cycle, clean spectra free from cancellation artefacts are acquired without the need to resort to gradient assisted coherence selection. A broad-band inversion ^{13}C pulse [17] applied in the middle of the $\text{BIRD}^{\text{r,X}}$ pulse eliminates losses of the signal caused by the relatively narrow inversion profile of rectangular 180° ^{13}C pulses.

After the transfer of magnetisation to ^{13}C via one-bond coupling constants the magnetisation evolves during a constant time interval, T , primarily under the influence of long-range coupling constants. A $\text{BIRD}^{\text{r,X}}$ is employed again, this time to separate the evolution due to $^1J_{\text{CH}}$ and $^nJ_{\text{CH}}$ during most of this interval [6,8].

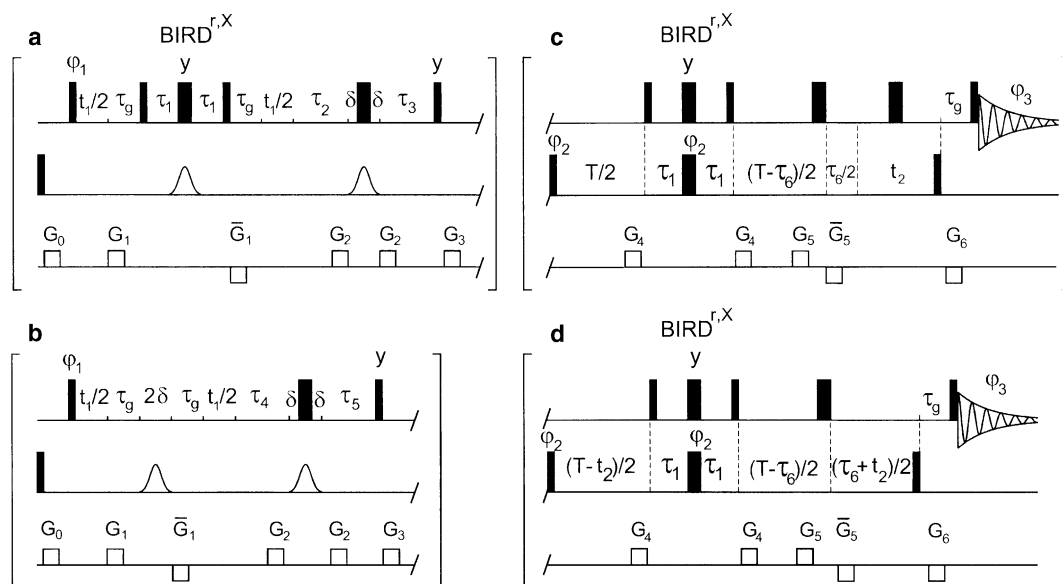


Fig. 1. HSQC (a, b) and HSQMBC (c, d) building blocks of the 3D HSQC-HSQMBC experiment. ^1H chemical shift labelling with (a) or without (b) the $\text{G-BIRD}^{\text{r,X}}$ pulse. Variable (c) or constant (d)-time ^{13}C chemical shift labelling. Thin and thick bars represent 90° and 180° non-selective pulses and are applied along the x -axis unless otherwise stated. The following two step phase cycle was applied: $\varphi_1 = x$; $\varphi_2 = x, -x$; $\varphi_3 = x, -x$. Phases φ_1 , φ_2 , and φ_3 were incremented according to STATES-TPPI in order to achieve sign discrimination in the indirectly detected periods. The initial sampling points in t_1 and t_2 were shifted by one half of the respective dwell times resulting in zero and first order phase corrections of 90° and -180° . The following delays were used: $\tau_1 = 1/2^1J_{\text{CH}}$, $\tau_2 = 1/2^1J_{\text{CH}} - \tau_g$, $\tau_3 = 1/2^1J_{\text{CH}} + \tau_g$, $\tau_4 = \tau_2 - \delta$, $\tau_5 = \tau_3 + \delta$, $\tau_6 = 1/2 * n^1J_{\text{CH}}$, where $n = 1$ for CH groups and $n = 2$ for CH_2 and CH_3 groups; τ_g includes a gradient of 1 ms and gradient recovery time of 0.2 ms; δ corresponds to half of the broad band carbon inversion pulse ($2\delta = 0.126$ ms). T is the $^nJ_{\text{CH}}$ evolution period. The strengths of gradients G_0 to G_6 were set to 10.0, 30.0, 11.6, 26.0, 16.0, 7.2, and 22.0 Gauss/cm, respectively. Gradients G_1 and \bar{G}_1 were applied along the z and y axes and the rest of the gradients were applied only along the z -axis.

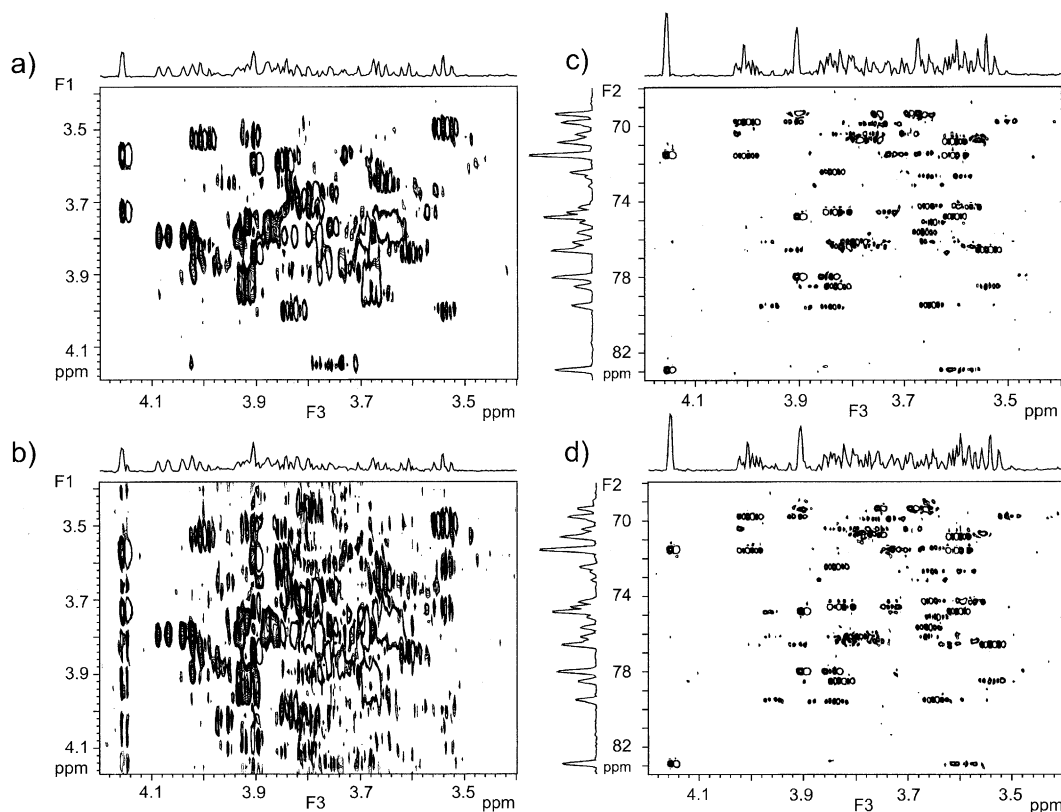


Fig. 2. 2D planes of the 3D HSQC-HSQMBC experiment acquired using the FNT pentasaccharide. The 2D spectra and their projections were plotted using the same vertical scale for each pair, and the threshold was set just above the white noise level. The (a) and (b) spectra were acquired using the pulse sequences of Fig. 1a+c and b+c, respectively. The carbon chemical-shift evolution period was kept constant. Note the cancellation artefact in spectrum (b). The (c) and (d) pair of spectra were acquired using the pulse sequences of Fig. 1a+c and a+d, respectively. The proton chemical-shift evolution period was kept constant. For parameters, see Section 3.

An additional 180° ^1H pulse applied $0.5\tau_6$ before the end of the T interval is required to refocus the one-bond coupling constants. In scheme of Fig. 1c, the magnetisation is labelled by ^{13}C chemical shifts during the following variable time period, t_2 , and is finally transferred back to long-range coupled protons by a pair of 90° pulses. Pure absorption proton multiplets in antiphase with respect the long-range proton–carbon coupling constants are detected during t_3 . The scheme shown in Fig. 1d combines the ^{13}C chemical shift labelling and the coupling evolution during the constant time interval T . This is achieved by gradually moving the BIRD cluster and a 180° ^1H pulse across the T interval. As a consequence, the $^nJ_{\text{CH}}$ coupling constants modulate the signal during t_2 . When the length of this interval is limited to times $< 0.5^nJ_{\text{CH}}$, no additional splitting is observed in F_2 as can be seen from the comparison of spectra in Fig. 2c and d. Nevertheless, for spin systems with many long-range couplings this could lead to broadening of signals. We therefore recommend the use of the variable-time chemical shift labelling of Fig. 1c as the relaxation effects during the variable t_2 interval can be neglected for medium size molecules.

The transfer efficiency of the 3D HSQC-HSQMBC pulse sequence depends mostly on the interplay between the passive and active long-range proton–carbon coupling constants as described by the following transfer function:

$$I = \sin^3(\pi^1J_{\text{CH}}\tau_1) \sin(\pi^1J_{\text{CH}}\tau_6) \cos^{n-1}(\pi^1J_{\text{CH}}\tau_6) \sin(\pi^nJ_{(\text{CH})\text{a}}(T - \tau_6)) \prod \cos(\pi^nJ_{(\text{CH})\text{p}}(T - \tau_6)) \exp(-T/T_{2\text{eff}}), \quad (1)$$

where $n = 1, 2, 3$ for CH, CH_2 , and CH_3 carbons, $T_{2\text{eff}}$ is the effective carbon spin–spin relaxation time, $^nJ_{(\text{CH})\text{a}}$ is the active long-range coupling constant and the product runs through all passive $^nJ_{(\text{CH})\text{p}}$. The sensitivity of the experiment is optimal for CH carbons ($\tau_6 = 0.5/{}^1J_{\text{CH}}$) and lower for CH_2 and CH_3 carbons ($\tau_6 = 0.25/{}^1J_{\text{CH}}$). The one bond correlation peaks are effectively suppressed when using $\tau_6 = 0.5/{}^1J_{\text{CH}}$, otherwise they will also appear in the spectra. In order to minimise the effect of passive long-range coupling constants, while at the same time allowing a significant amount of antiphase magnetisation with respect to the active long-range coupling to be created, the constant time interval is kept below 50 ms.

When considering a CH carbon with $^1J_{\text{CH}} = 145$ Hz, an active long-range coupling constant, $^nJ_{(\text{CH})\text{a}} = 5.0$ Hz, two passive couplings, $^nJ_{(\text{CH})\text{p}} = 5.0$ and 2.5 Hz, $T = 50$ ms and $\tau_1 = \tau_6 = 0.5/{}^1J_{\text{CH}}$ optimised for ${}^1J_{\text{CH}} = 155$ Hz, the transfer efficiency of the 3D HSQC-HSQMBC pulse sequence as given by Eq. (1) is 45%. A similar analysis was performed using the pulse sequence of the 3D long-range correlation experiment proposed by Hernández and LeMaster [4], using an identical spin system and parameters recommended by the authors. Two proton–proton coupling constants of 8 and 10 Hz, which in this experiment also contribute to the cross peak intensities in spectra of carbohydrates, were included in the calculations. The obtained transfer efficiency was 11%, which incorporated the sensitivity enhancement by factor of 1.4 for CH carbons. For α and β anomeric carbon resonances, additional factors of 0.47 and 0.35 must be considered due to the difference between the anomeric ${}^1J_{\text{CH}}$ couplings constants (170 and 160 Hz) and the one (145 Hz) used to optimise the long-range evolution interval (27.4 ms). A clear advantage of this experiment is that the cross peaks are in all its di-

mensions in-phase, while they are in antiphase in the directly detected dimension of the proposed 3D HSQC-HSQMBC experiment. Antiphase peaks can have reduced intensities, depending on the interplay between J_{HH} and ${}^nJ_{\text{CH}}$ coupling constants and the spin–spin relaxation times. Theoretical simulations, using typical coupling constants of oligosaccharides, show that this effect can result in signal reduction of up to 50%.

Using the pulse sequence of Fig. 1a+c the 3D HSQC-HSQMBC experiment is illustrated using a 5 mM pentasaccharide sample. Given the narrow range of carbohydrate resonances it was possible to acquire a 3D spectrum in 27 h, with a digital resolution typically used for 2D experiments. Advantage was taken of the fact that ${}^1\text{H}$ and ${}^{13}\text{C}$ signals of anomeric atoms resonate in separate spectral regions from the rest of carbohydrate resonances and anomeric carbons were folded in F_2 (see HSQC spectrum in Fig. 3a) without introducing any ambiguity. Fig. 3b and c show the F_2F_3 and F_1F_3 projections of the 3D spectrum. The ability of the HSQC-HSQMBC experiment to separate the long-range correlation cross peaks is best illustrated by inspecting

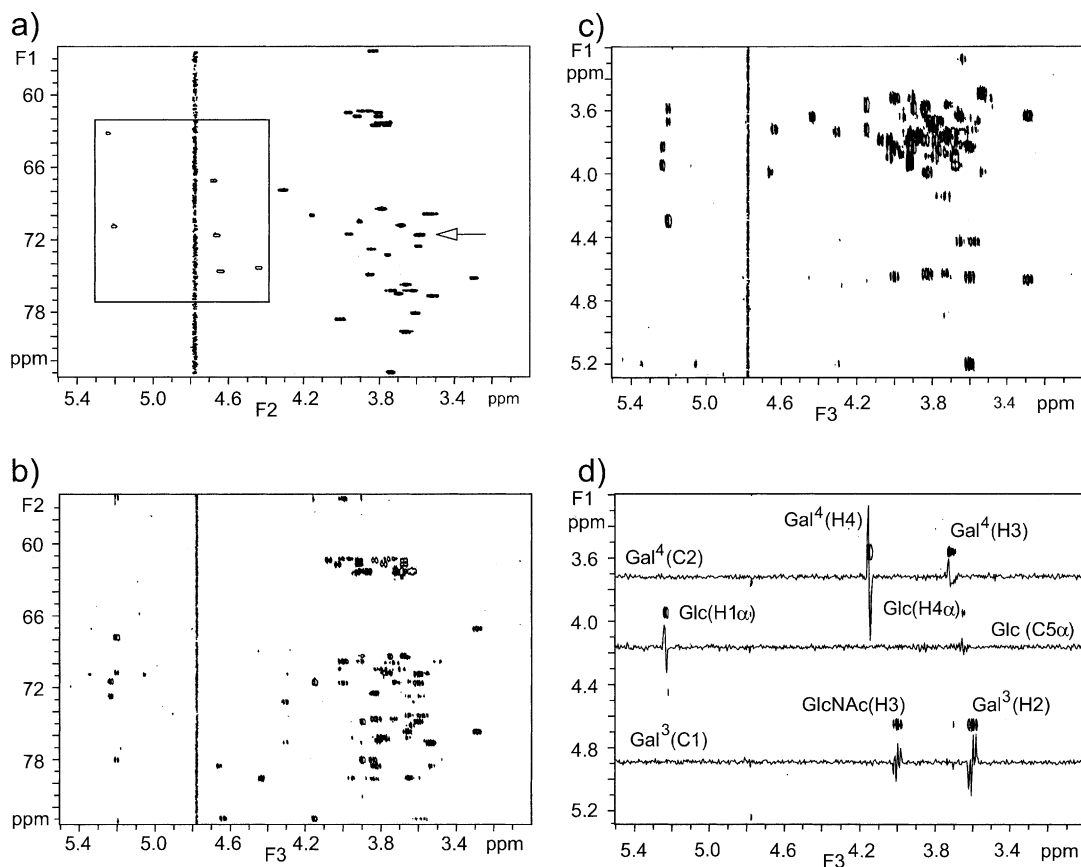


Fig. 3. 3D HSQC-HSQMBC experiments on the FNT pentasaccharide. Negative cross peaks were plotted using one contour only. (a) 2D HSQC, the cross peaks of anomeric signals folded in F_1 are surrounded by a box; (b) and (c) show the F_2F_3 and F_1F_3 projections of the 3D spectrum; (d) F_1F_3 plane taken at the ${}^{13}\text{C}$ chemical shift indicated by arrows in the spectrum (a). The superscript in cross peak annotations refers to glycosidic linkages of individual residues. Cancellation artefacts at 4.78 ppm originate from an intense HOD signal. For parameters see Section 3.

the F_1F_3 planes. In addition to the editing of proton signals by the ^{13}C chemical shift of long-range coupled carbons in F_2 , the cross peaks in F_1F_3 are separated in F_1 by the chemical shifts of protons directly attached ^{13}C atoms. The F_1F_3 plane (Fig. 3d) taken at the position indicated by an arrow shown in the HSQC spectrum of Fig. 3a. contains long-range proton–carbon cross peaks of three carbons. Two of those, Gal⁴(C2) and Glc(C5 α), differ in their chemical shifts only by 0.06 ppm while the third set of cross peaks belongs to the folded anomeric carbon Gal³(C1). Note that the opposite phase of the Gal³(C1) cross peaks is due to the folding of this carbon in the F_2 dimension.

3. Experimental

All spectra were acquired using 2 mg of a FNT pentasaccharide, α -Fuc-(1 \rightarrow 2)- β -Gal-(1 \rightarrow 3)- β -GlcNAc-(1 \rightarrow 3)- β -Gal-(1 \rightarrow 4)-Glc, dissolved in 0.55 ml of D_2O at 25 °C. The 3D spectrum (Fig. 3) was acquired using the following parameters. Intervals τ_1 and τ_6 (3.23 ms) were optimised for CH groups and $^1J_{\text{CH}}$ of 155 Hz. The $^nJ_{\text{CH}}$ evolution period T was set to 50 ms. Number of increments in F_1 and F_2 was 64 and 128, respectively. The sweep widths in t_1 , t_2 , and t_3 were 1500, 4526, and 1500 Hz yielding corresponding acquisition times of 42.6, 28.3, and 341 ms, respectively. A relaxation delay of 1 s was used. Two scans were acquired per increment resulting in a total acquisition time of 27 h. The HOD signal was not presaturated. The spectrum was zero-filled once in both indirectly detected dimensions. The F_1F_3 and F_2F_3 planes shown in Fig. 2 were acquired by using 64 scans per increment. All the other parameters were identical to those used to acquire the 3D spectrum. The overall acquisition times were 3.3 and 6.5 h for the proton–proton and proton–carbon planes, respectively.

4. Conclusion

The main feature of the proposed 3D HSQC-HSQMBC experiment is its ability to spread the long-range correlation cross peaks along an additional ^1H dimension thus providing separation of signals not achievable by standard 2D long-range correlation methods with only a ^{13}C indirectly detected dimension. The experiment is designed for protonated systems and does not yield long-range correlation of quaternary carbons. It is aimed at complex molecules with many protonated carbons exhibiting a narrow spread of ^{13}C chemical shifts e.g., complex carbohydrates. Evolution of single-quantum coherences throughout the entire pulse sequence ensures that the cross peaks are inphase pure absorption singlets in both indirectly detected dimensions, thus maximising the resolution and sensitivity

of the experiment. The antiphase character of peaks in the directly detected dimension could cause some signal attenuation for molecules with increased proton line widths and/or smaller coupling constants. The cross peak intensities are affected by both active and passive long-range coupling constants, and in the case of CH_2 and CH_3 carbons also by one-bond proton–carbon coupling constants. Nevertheless, as demonstrated in this paper, high quality spectra can be accumulated using millimolar concentration of samples and modest experimental times. The technique is also suitable for measurement of long-range heteronuclear coupling constants from the pure antiphase multiplets in the directly detected dimension.

References

- [1] L. Müller, Sensitivity enhanced detection of weak nuclei using multiple-quantum coherence, *J. Am. Chem. Soc.* 101 (1979) 4481–4484.
- [2] G. Bodenhausen, D.J. Ruben, Natural abundance nitrogen-15 NMR by enhanced heteronuclear spectroscopy, *Chem. Phys. Lett.* 69 (1980) 185–189.
- [3] B.L. Marquez, W.H. Gerwick, R.T. Williamson, Survey of NMR experiments for the determination of $^nJ(\text{C},\text{H})$ heteronuclear coupling constants in small molecules, *Magn. Reson. Chem.* 39 (2001) 499–530.
- [4] G. Hernández, D.M. LeMaster, 3D heteronuclear long-range ^1H – ^{13}C scalar correlation at natural abundance: application to oligosaccharide analysis, *Magn. Reson. Chem.* 40 (2002) 169–174.
- [5] T.J. Norwood, J. Boyd, N. Soffe, J.D. Campbell, New nuclear-magnetic-resonance technique for determining long-range heteronuclear ^1H – ^{15}N correlations in proteins, *J. Am. Chem. Soc.* 112 (1990) 9638–9640.
- [6] D. Uhrin, A. Mele, J. Boyd, M.R. Wormald, R.A. Dwek, New methods for measurement of long-range proton–carbon coupling-constants in oligosaccharides, *J. Magn. Reson.* 97 (1992) 411–418.
- [7] K.V.R. Chary, G. Otting, K. Wütrich, *J. Magn. Reson.* 93 (1991) 218–224.
- [8] L. Poppe, H. van Halbeek, ^1H -detected measurement of long-range heteronuclear coupling constants. Application to a trisaccharide, *J. Magn. Reson.* 92 (1991) 636–641.
- [9] B. Adams, L. Lerner, Measurement of long-range ^1H – ^{13}C coupling constants using selective excitation of carbon-13, *J. Magn. Reson. A* 103 (1993) 97–102.
- [10] S. Mattila, A.M.P. Koskinen, G. Otting, Long-range HSQC with spin-lock purge pulses for observation of heteronuclear correlations with ^1H detection and low t_1 noise, *J. Magn. Reson. B* 109 (1995) 326–328.
- [11] R.T. Williamson, B.L. Marquez, W.H. Gerwick, K.E. Kövér, One- and two-dimensional gradient-selected HSQMBC NMR experiments for the efficient analysis of long-range heteronuclear coupling constants, *Magn. Reson. Chem.* 38 (2000) 265–273.
- [12] J.R. Garbow, D.P. Weitekamp, A. Pines, Bilinear rotation decoupling of homonuclear scalar interactions, *Chem. Phys. Lett.* 93 (1982) 504–509.
- [13] A. Bax, Broad-band homonuclear decoupling in heteronuclear shift correlation NMR spectroscopy, *J. Magn. Reson.* 53 (1983) 517–520.
- [14] G. Mackin, A.J. Shaka, Phase-sensitive two-dimensional HMQC and HMQC-TOCSY spectra obtained using double

- pulsed-field-gradient spin echoes, *J. Magn. Reson. A* 118 (1996) 247–255.
- [15] D. Uhrín, G. Batta, V.J. Hruby, P.N. Barlow, K.E. Kövér, Sensitivity and gradient-enhanced hetero (ω_1) half-filtered TOCSY experiment for measuring long-range heteronuclear coupling constants, *J. Magn. Reson.* 130 (1998) 155–161.
- [16] A. Bax, S.S. Pochapsky, Optimized recording of heteronuclear multidimensional NMR spectra using pulsed field gradients, *J. Magn. Reson.* 99 (1992) 638–643.
- [17] M.A. Smith, H. Hu, A.J. Shaka, Improved broadband inversion performance for NMR in liquids, *J. Magn. Reson.* 151 (2001) 269–283.